Mechanics and Mechanical Engineering
Vol. 20, No. 4 (2016) 499–513

Thermo–Mechanical Deformation and Stress Analysis of Hydroxyapatite/Titanium FGM plate by FEM

Rajesh Sharma
Research Scholar
I.K. Gujral Punjab Technical University
Jalandhar, India
raz_867@yahoo.com

V. K. Jadon
Chitkara University Rajpura
Punjab. India

Balkar Singh
I.K. Gujral Punjab Technical University
Jalandhar, India

Received (23 September 2016)
Revised (16 November 2016)
Accepted (15 December 2016)

Hydroxyapatite(HA)/titanium(Ti) functionally graded materials(FGM) are latest materials used for medical implants, structural components in defense, in dentistry, in aviation, and other fields under various type of loads. A finite element analysis model is designed to study the behavior of a HA/Ti FGM plate under thermo-mechanical loadings. Simply supported plate subjected to mechanical and thermal loads on its top and bottom surface is considered with suitable temperature and loading function. The first-order shear deformation plate (FSDT) method is used to investigate the thermo mechanical behavior of functionally graded plate .The volume fraction of the FGM plate is varied smoothly and continuously along the thickness of the plate. Results are discussed for the deformation and stresses of HA/Ti FGM plate It is observed from the study that FGMs are able to resist higher temperatures and loads without delamination.

Keywords: functionally graded material (FGM); finite element method (FEM); thermo–mechanical analysis.

1. Introduction

Functionally graded materials (FGM) are composite materials, in which the volume constituent of the material is chosen as a variable function of the material position in thickness dimensions of the structure. FGM materials find applications in high temperature environments. These materials helps in reducing thermal stresses and

perform well in high temperature conditions [1].To reduce stress and resist super high temperature, they have continuous transition from metal at low temperature surfaces to ceramics at high temperature surfaces. FGMs are used in high temperature environments such as aviation and nuclear reactor. So it is necessary to analyze the temperature and thermal stress field of the functionally graded materials. Yangjian et. al. [2] researched the effect of FGM layer thickness on temperature field by finite element method. In their research they concluded that with increase in FGM layer thermal stresses reduced to a safe limit. R. Ramkumar and N. Ganesan [3] studied the problem of buckling in thin walled box columns under thermal environment by using CLPT theory; and developed software for finding buckling of columns. Chen and Tong [4] used a graded finite element approach to analyze the sensitivity in the problems of steady state and transient heat conduction in FGMs. It is concluded in their study that optimization of properties of FGM helps to analyze the sensitivity. Alshorbagy et al. [5] concluded that FGM plate provides high ability to withstand thermal stresses under thermo-mechanical loads. Thermal analysis of FGM plates are reported in [6-9] First-order shear deformation theory (FSDT) is used to study mechanical and thermal bending analysis of FGM plates in [10–12].

Analytical methods are also used to study thermo elastic behavior [13–16]. Analytical methods can be used for simple geometries but they are difficult for complex geometries and time consuming. Reddy et. al.[17] investigated thermo-mechanical deformations in FGM plates, they discovered that FGM plates are able to work well loads under thermo–mechanical loadings with comparison to composite plates. Thermal stress analysis in functionally graded materials using high–order control volume FEM is proposed in [18], they concluded that thermal stresses reduces in FGM region. Mine Uslu [19] reports that volume fraction parameter from 0.2 to 0.5 provides the optimum solution to thermally loaded plates.

In HA/Ti functionally graded materials titanium is used as bio-inert load wearing element for making core of medical implants and coupled with hydroxyapatite (HA), which has bioactive functional properties used at the surface as ceramic constituent using a FGM approach[20]. This combination avoid spoliation and metal ion dissolution into blood stream where the composition is gradually varied from a metallic core region to a bio–ceramic rich surface region without an abrupt interface, the mechanical properties, biological properties, and lifespan of the component are expected to improve drastically.

In this paper the authors investigated HA/Ti FGM plate and its behavior under different loading conditions. The mechanical, thermal, and coupled thermo–mechanical behavior of HA/Ti FGMs will be investigated. The results of developed model are verified and compared with available literature. The results obtained are shown in the form of figures and tables to present the effect of volume fraction and load response of the plate. This investigation is a benchmark for advanced research work. These results are significant for developing thermal barrier materials. Finite element method is used for the analysis using first–order shear deformation theory (FSDT).

2. Theoretical development and formulation

HA/Ti plate with non homogeneous thermal and material properties in thickness direction is taken as shown in Fig. 1.

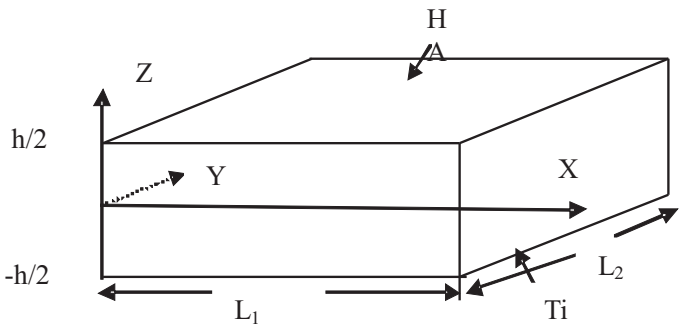

Figure 1 HA/Ti FGM plate with top surface made of HA and bottom surface of Ti

The change in temperature of the elastic body due to elastic deformations, and the inertia term in the equations of motion are neglected. Material properties varied in the thickness direction according to volume fraction power law distribution such that top layer is made up of ceramic and graded to metal at the bottom surface. The volume fraction is expressed as:

$$V_c(z) = \left(\frac{2z+h}{2h}\right)^n \tag{1}$$

where n is the volume fraction index. Temperature field is assumed to vary in thickness direction such that is $\mathrm{dT/dx} = \mathrm{dT/dy} = 0$. The heat conduction equation in FGM, using continuous material properties along thickness, can be written as:

$$\frac{d}{dt}\left(k\,(z)\,\frac{dT}{dt}\right) \;\; = \; 0 \tag{2}$$

$T(z)$ is the temperature distribution through z direction and k *(z)* is the variable thermal conductivity [21], so:

$$T(z) = T_c - \frac{T_c - T_m}{\int_{-h/2}^{h/2}(dz/k(z))}\int_z^{-h/2} dz/k(z) \tag{3}$$

where

$$k(z) = (k_c - k_m)\left(\frac{2z+h}{2h}\right)^n + k_m$$

Table 1 Material properties of HA/Ti FGM plate

Property	Titanium	Hydroxyapatite
Thermal conductivity	17.52 kW/mK	2.16 kW/mK
Thermal expansion	10.9x10^{-6}/?C	14.87x10^{-6}/?C
Poisson's ratio	0.34	0.28
Young's modulus	116 GPa	73 GPa

and the thermal boundary conditions are imposed as:

$$T = T_c atz = +h/2 \tag{4}$$
$$T = T_m atz = -h/2 \tag{5}$$

Thermo–physical material properties are given in Tab. 1. The temperature of the top surface (ceramic) is 300^{o}C and the temperature of the metal rich bottom surface is 20^{o}C.

3. Finite element formulation

Displacement fields for FGM are taken as:

$$\begin{aligned} u(x,y,z) &= u_0(x,y) + (z)\theta_x(x,y) \\ v(x,y,z) &= v_0(x,y) + (z)\theta_y(x,y) \\ \omega(x,y,z) &= \omega_0(x,y) \end{aligned} \tag{6}$$

where (u_0, v_0, ω_0, θ_x, θ_y) are unknown functions to be determined.
So lagrange strain components for small deformations and rotations can be found from as:

$$\begin{aligned} e_{xx} &= u_{0,x} + (z)\theta_{xx} \\ e_{yy} &= u_{0,y} + (z)\theta_{yy} \\ \gamma_{xy} &= u_{0,y} + (z)(\theta_{x,y} + \theta_{y,x}) \\ \gamma_{xz} &= \omega_{0,x} + \theta_{x,} \\ \gamma_{yz} &= \omega_{0,y} + \theta_{y,} \end{aligned} \tag{7}$$

further

$$e_{ij} = \varepsilon_{ij} + \varepsilon_{Ti} \tag{8}$$

where e_{ij} are the total strain components, ε_{ij} elastic strains, and ε_{Ti} are thermal strains.
Thses can also be written as:

$$\left\{ \begin{array}{c} e_{xx}(x,y,z) \\ e_{yy}(x,y,z) \\ \gamma_{xy}(x,y,z) \end{array} \right\} = \left[\begin{array}{cccccc} 1 & 0 & 0 & z & 0 & 0 \\ 0 & 1 & 0 & 0 & z & 0 \\ 0 & 0 & 1 & 0 & 0 & z \end{array} \right] X \left[\begin{array}{c} u_{0,x}(x,y) \\ v_{0,y}(x,y) \\ u_{0,y}(x,y) + v_{0,x}(x,y) \\ \theta_{x,x}(x,y) \\ \theta_{y,y}(x,y) \\ \theta_{x,y}(x,y) + \theta_{y,xz}(x,y) \end{array} \right] \tag{9}$$

or

$$\{e_b\} = [Z_b]\left\{e_b^0\right\} \tag{10}$$

where is $\{e_b{}^0\}$ nodal bending strain.
Using principle of minimum potential energy as

$$\pi = \left(0.5\int_A \left\{e_b^0\right\}^T [DE_b]\left\{e_b^0\right\} dA - \int_A \left\{e_b^0\right\}^T [DT_b]\, dA\right) - \sum \{P\}\left\{u^0\right\} \tag{11}$$

where

$$\begin{gathered}[DT_b] = \int_z [Z_b]^T [D_b]^T \{\varepsilon_{Tb}\}\, dz \\ \{\varepsilon_{Tb}\} = \left\{ \begin{array}{c} \alpha(z)\delta T(z) \\ \alpha(z)\delta T(z) \\ 0 \end{array} \right\}\end{gathered} \tag{12}$$

where $\alpha(z)$ is the thermal coefficient of expansion and $\delta T(z)$ is the continuum temperature change through the plate thickness.
By integrating the material properties through plate thickness we get single layer matrix as:

$$[DE_b] = \int_{-h/2}^{h/2} [Z_b]^T [D_b]^T [Z_b]\, dz \tag{13}$$

where $[D_b]$ is bending material matrices. It provides the stress–strain relations for FGM plate, which are given below.

$$[DE_b] = \left[\begin{array}{ccc} \overline{Q_{11}} & \overline{Q_{12}} & \overline{Q_{16}} \\ \overline{Q_{11}} & \overline{Q_{22}} & \overline{Q_{26}} \\ \overline{Q_{16}} & \overline{Q_{26}} & \overline{Q_{66}} \end{array} \right] \tag{14}$$

The equivalent material matrix can also be written as

$$[DE_b] = \left[\begin{array}{cc} A_{ij} & B_{ij} \\ B_{ij} & D_{ij} \end{array} \right] \tag{15}$$

where A_{ij} are the extensional stiffness components, B_{ij} are bending-extensional coupling stiffness components, and D_{ij} are the bending stiffness components.

$$A_{ij} = \int_{-h/2}^{h/2} \overline{Q_{ij}}(z)dz \qquad i,j = 1,2,6 \tag{16}$$

$$B_{ij} = \int_{-h/2}^{h/2} z\overline{Q_{ij}}(z)dz \qquad i,j = 1,2,6 \tag{17}$$

$$D_{ij} = \int_{-h/2}^{h/2} z^2\overline{Q}(z)dz \qquad i,j = 1,2,6 \tag{18}$$

$\overline{Q_{ij}}(z)$ are the equivalent material property stiffness as a function of the material thickness direction z.

The equivalent material stiffness of isotropic FGM plate is

$$\begin{array}{l}\overline{Q_{11}}(z)=\overline{Q_{22}}(z)=\frac{E(z)}{1-v^2}\overline{Q_{12}}(z)=v\overline{Q_{11}}(z)\\ \overline{Q_{66}}(z)=\frac{1-v}{2}\overline{Q_{11}}(z)\\ \overline{Q_{44}}(z)=\overline{Q_{55}}(z)=K\frac{1-v}{2}\overline{Q_{11}}(z)\\ \overline{Q_{16}}(z)=\overline{Q_{26}}(z)=\overline{Q_{45}}(z)=0\end{array} \tag{19}$$

The normal rotations and deflection at any point in FGM plate having n nodes of the element are

$$\begin{array}{l}\left\{\begin{array}{c}u_0(x,y)\\ v_0(x,y)\\ \omega_0(x,y)\\ \theta_x(x,y)\\ \theta_y(x,y)\end{array}\right\}=\sum_{i=1}^{n}\left[\begin{array}{ccccc}\psi_{i,x}^e & 0 & 0 & 0 & 0\\ 0 & \psi_{i,y}^e & 0 & 0 & 0\\ \psi_{i,y}^e & \psi_{i,x}^e & 0 & 0 & 0\\ 0 & 0 & 0 & \psi_{i,x}^e & 0\\ 0 & 0 & 0 & 0 & \psi_i^e\end{array}\right]\left\{\begin{array}{c}u_j\\ v_j\\ \omega_j\\ \theta_j\\ \theta_j\end{array}\right\}\\ \left\{e_b^0\right\}=\sum_{i=1}^{n}\left[B_{bi}\right]\left\{u_j^0\right\}\end{array} \tag{20}$$

where ψ_i^e is the lagrange interpolation function at node i.
The nodal bending strain can be written as follows

$$\left\{e_b^i\right\}=\left[\begin{array}{c}u_{0,x}(x,y)\\ v_{0,y}(x,y)\\ u_{0,y}(x,y)+v_{0,x}(x,y)\\ \theta_{x,x}(x,y)\\ \theta_{y,y}(x,y)\\ \theta_{x,y}(x,y)+\theta_{y,xz}(x,y)\end{array}\right] \tag{21}$$

$$=\sum_{i=1}^{n}\left[\begin{array}{ccccc}\psi_{i,x}^e & 0 & 0 & 0 & 0\\ 0 & \psi_{i,y}^e & 0 & 0 & 0\\ \psi_{i,y}^e & \psi_{i,x}^e & 0 & 0 & 0\\ 0 & 0 & 0 & \psi_{i,x}^e & 0\\ 0 & 0 & 0 & 0 & \psi_{i,y}^e\\ 0 & 0 & 0 & \psi_{i,y}^e & \psi_{i,x}^e\end{array}\right]\left\{\begin{array}{c}u_i\\ v_i\\ \omega_i\\ \theta_i\\ \theta_i\end{array}\right\} \tag{22}$$

$$\text{or } \left\{e_b^0\right\}=\sum_{i=1}^{n}\left[B_{bi}\right]\left\{u_i^0\right\}$$

where $[B_{bi}]$ is the curvature displacement matrix and $\left\{u_i^0\right\}$ are nodal degrees of freedom.
So the potential energy can be obtained and equation (23) can be written as:

$$\begin{array}{l}\pi=\left(0.5\int_A\left\{u^0\right\}^T\left[B_b\right]^T\left[DE_b\right]\left[B_b\right]\left\{u^0\right\}dA\right)\\ -\int_A\left\{u^0\right\}^T\left[B_b\right]^T\left\{DT_b\right\}dA-\sum_{i=1}^{n}\left\{u^0\right\}^T\left\{p\right\}=0\end{array} \tag{23}$$

The minimum potential energy principle states that:

$$\delta\pi=\left(\int_A\left[B_b\right]^T\left[DE_b\right]\left[B_b\right]dA\right)\left\{u^0\right\}-\int_A\left\{DT_b\right\}dA-\sum_{i=1}^{n}\left[\psi_i^e\right]^T\left\{p\right\}=0 \tag{24}$$

In another form

$$[K_b]\left\{u^0\right\} = \{F_T\} + \{P\} \tag{25}$$

$[K_b]$ is stiffness matrix $\{F_T\}$ and $\{P\}$ are the element thermal and mechanical load vectors, respectively, defined as

$$\begin{aligned}
[K_b] &= \int_A [B_b]^T [DE_b] [B_b]\, dA \\
\{P\} &= \int_A [\psi_i^e]^T \{p\}\, dA \\
\{F_T\} &= \int_A [B_b]^T \{DT_b\}\, dA
\end{aligned}$$

Now by putting (20) into (9) the bending strain matrix will be obtained. The stress components can be evaluated as:

$$\begin{Bmatrix} \sigma_{xx} \\ \sigma_{yy} \\ \sigma_{xy} \end{Bmatrix} = \begin{bmatrix} \overline{Q_{11}}(z) & \overline{Q_{12}}(z) & 0 \\ \overline{Q_{12}}(z) & \overline{Q_{22}}(z) & 0 \\ 0 & 0 & \overline{Q_{66}}(z) \end{bmatrix}$$

$$X \left\{ \begin{Bmatrix} e_{xx} \\ e_{yy} \\ \gamma_{xy} \end{Bmatrix} - \begin{Bmatrix} \alpha(z)\delta T(z) \\ \alpha(z)\delta T(z) \\ 0 \end{Bmatrix} \right\} \tag{26}$$

or:

$$\{\sigma_b\} = [D_b]\{\varepsilon_b\} \tag{27}$$

4. Solution scheme

A simulation scheme with coding in Visual C++ is used for the study. In first of all, temperatures at the nodes are calculated. Visual C++ solver coded in C++ is used to generate thermal stiffness matrix and thermal load vector using the thermo-mechanical equations derived in previous section. After that in assembly part total structural stiffness matrix and structure load vector of total elements are generated. Required boundary conditions are applied. In last part we get solution in terms of deflection and stress.

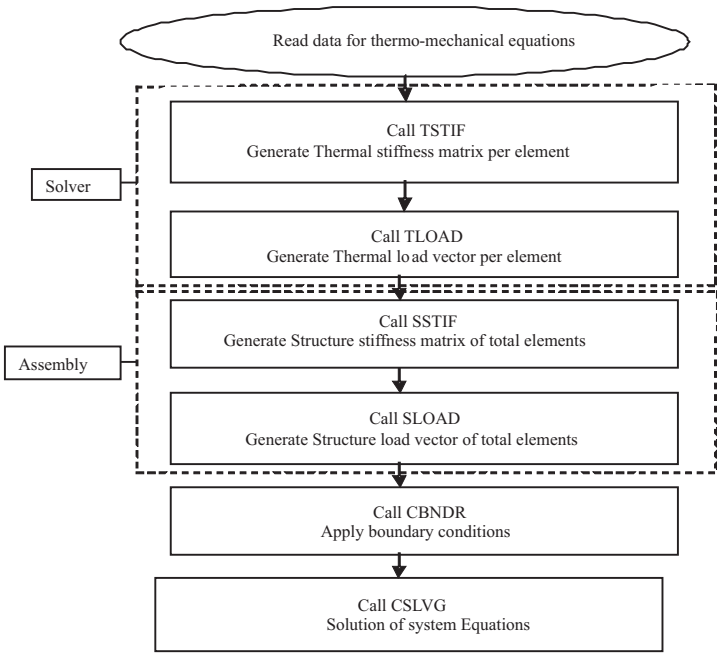

Figure 2 Flow chart of Finite element modeling of HA/Ti FGM plate

5. Numerical results

The validation of the proposed model is examined by comparing the results with the available literature. An eight noded isoparemetric element with 12 degrees of freedom per node for the model has been used for the analysis of HA/Ti FGM plate. Mechanical and thermal loadings are imposed on the plate under consideration.

5.1. *Validation study*

The validation of the thermo–mechanical analysis is carried out. Table 2 shows deflection results of Ni/ZrO_2FGM plate. The developed model gives consistent results with Reddy et al. [17]. The results of Al/Zro_2 FGM plate with mechanical and thermo-mechanical loadings are shown in Tab. 3 and 4. The results are comparable with the Alshorbagy et al. [5]. The results of the present study are more precise and close to actual values as compared to [5, 17 and 22].

5.2. *Temperature distribution in FGM Plate without heat source*

The temperature distribution is a function of material parameter(volume fraction index) n as shown in Fig. 3,with the change in the value of n the temperature distribution becomes non linear. The temperature distribution in FGM plates is smaller than those of homogeneous plates, which are made up of purely ceramic and metallic materials. The grading parameter n has dominant effect on the thermal

analysis of the FGM plates, where the temperature distribution depends on the variable thermal conductivity of the FGM.

5.3. *Deformation of FGM plate under Mechanical Loading*

Ti at the bottom and HA at the top of the plate is chosen, to investigate the thermo elastic behavior of plate. Several numerical simulations are carried out, for different values of the grading parameter n. The following non dimensional parameters are used throughout the numerical simulations.

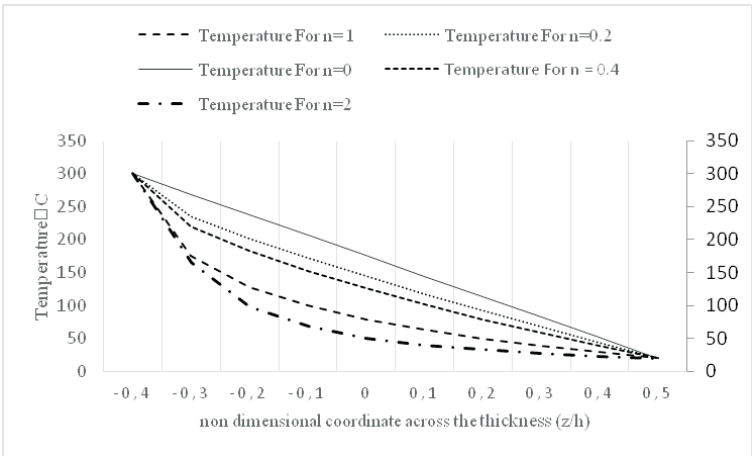

Figure 3 Temperature through the FGM plate thickness for different values of n without heat source

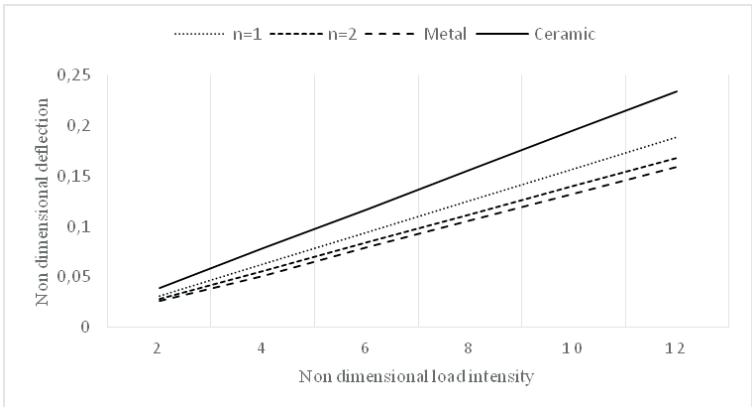

Figure 4 Non dimensional central deflection of FG plate versus non dimensional load intensity.

Non dimensional load intensity $\bar{P}$ =L^4p/E_mh^4;

Central deflection $\bar{w}$= w/h,

Thickness $\bar{h}$= h/L

Where p is load intensity and E_m is the young's modulus of the Aluminum bottom face. It can be noticed from Fig. 4 that the deformation decreases by increasing the volume fraction index (n). As the material changes from metal to ceramic from bottom to top face of the FGM plate the rigidity of the material increases because ceramic are more rigid than metals. Deflection of FGM plate with different grading parameter is also shown in Table 5.

Table 2 Deflection and normal stress of Ni/ZrO_2 plate under thermal loads

Parameter	Temp. z/h=0	In–plane displacement			Transverse displacement			Normal stress		
z/h		0	0.5	1	0	0.5	1	0	0.5	1
J.N.Reddy et.al.(2001)	0.2432	0.0849	-0.786	-1.696	5.521	5.631	6.022	-75.54	-242	-1005
Developed model	0.2561	0.0796	-0.715	-1.601	5.412	5.601	5.992	-75.32	-245	-998

Table 3 Deflection under mechanical loads of Al/ZrO_2 FGM plate

$\bar{P}$	Metal		n=1		n=2		Ceramic	
	Developed model	Established*	Developed model	Established*	Developed model	Established*	Developed model	Established*
1	0.0451	0.0452	0.0286	0.0287	0.0327	0.0267	0.0210	0.0210
2	0.0901	0.0905	0.0583	0.0573	0.0653	0.0534	0.0418	0.0420
3	0.1348	0.1357	0.0886	0.0860	0.0988	0.0801	0.0626	0.0629
4	0.1793	0.1810	0.1185	0.1146	0.1306	0.1067	0.0834	0.0839
5	0.2251	0.2262	0.1474	0.1433	0.1635	0.1334	0.1042	0.1049
6	0.2689	0.2714	0.1781	0.1720	0.1965	0.1601	0.1251	0.1258
7	0.3148	0.3167	0.2090	0.2006	0.2280	0.1868	0.1466	0.1468
8	0.3601	0.3619	0.2367	0.2293	0.2611	0.2135	0.1674	0.1678
9	0.4045	0.4072	0.2665	0.2579	0.2937	0.2402	0.1873	0.1888
10	0.4488	0.4524	0.2962	0.2899	0.3263	0.2669	0.2081	0.2097

* Alshorbagy et al. [5]

5.4. *Deformation of FGM plate under thermo–mechanical loading*

The deflection due to a series of mechanical loads for different values of grading parameter n is shown in Fig. 5. In addition to the uniformly distributed load on the top surface, the plate is subjected to a thermal load where the ceramic rich top surface is held at 300^oC and metal rich bottom surface is held at 20^oC.

Table 4 Deflection of Al/ZrO_2 FGM plate under thermo-mechanical loads

$\bar{P}$	Metal		n=1		n=2		Ceramic	
	Developed model	Established*	Developed model	Established*	Developed model	Established*	Developed model	Established*
1	-0.2014	-0.2050	-0.0598	-0.0665	-0.0581	-0.0547	-0.0862	-0.0879
2	-0.1566	-0.1598	-0.0331	-0.0379	-0.0253	-0.0280	-0.0655	-0.0669
3	-0.1118	-0.1146	0.0086	-0.0092	0.0011	-0.0013	-0.0447	-0.0459
4	-0.0672	-0.0690	0.0183	0.0195	0.0220	0.0254	-0.0240	-0.0250
5	-0.0222	-0.0240	0.0420	0.0481	0.0502	0.0521	-0.0035	-0.0040
6	0.0224	0.0210	0.0727	0.0768	0.6912	0.0788	0.0174	0.0170
7	0.0668	0.0660	0.1028	0.1054	0.1021	0.1054	0.0382	0.0380
8	0.1121	0.1115	0.1251	0.1341	0.1254	0.1321	0.0591	0.0589
9	0.1567	0.1568	0.1548	0.1628	0.1457	0.1588	0.0797	0.0799
10	0.2018	0.2020	0.1845	0.1914	0.1745	0.1855	0.1004	0.1009

* Alshorbagy et al. [5]

Table 5 Deflection of FGM plate with different grading parameter

Load Intensity	n=1	n=2	n=0.5	Ceramic(HA)	Metal(Ti)
	Central Deflection	Central Deflection	Central Deflection	Central Deflection	Central Deflection
2	0.0314	0.0280	0.0263	0.0390	0.0910
4	0.0628	0.0561	0.0527	0.0780	0.1833
6	0.0942	0.0841	0.0790	0.1170	0.2750
8	0.1256	0.1122	0.1054	0.1560	0.3666
10	0.1570	0.14025	0.1317	0.1950	0.4583
12	0.1884	0.1683	0.1581	0.2340	0.5500

It can be observed from figure that materials having properties in between ceramic and metal constituents shows intermediate values of deflection. This was expected as the metallic plate is one with minimum stiffness and ceramic plate with maximum stiffness.

5.5. *Axial stresses in FGM plate under thermo–mechanical loading*

The variation of axial stresses at the centre of FGM plate along the thickness direction for different values of grading factor n is shown Fig. 6. The maximum tensile stresses along the thickness of FGM plates are located at the bottom edge and increases with the increase in modular ratio.

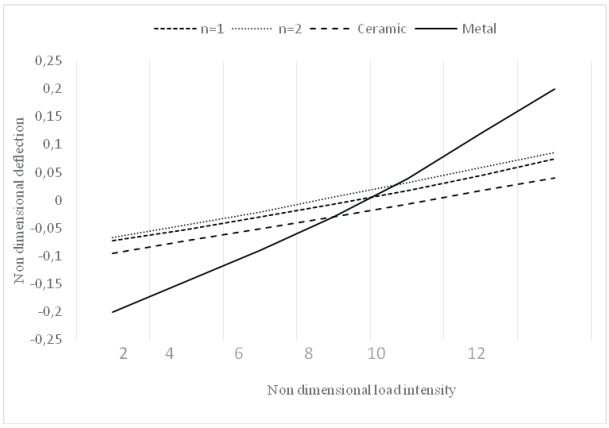

Figure 5 Deflection of HA/Ti FGM plate due to thermo–mechanical load

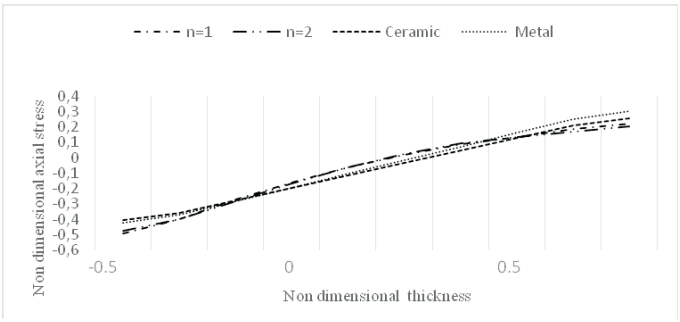

Figure 6 Axial stresses due to thermo mechanical load

5.6. *Deformation of FGM plate under varying heat source strength*

While increasing the value of grading parameter n, the FGM plate becomes more sensitive for the amount of heat delivered from the heat source. Figure 7 shows deflection of FGM plate due to sequence of mechanical loads for different values of n. Fig. 8 shows the non dimensional deflection of the FGM plate versus the heat source strength. In FGM plate, it is observed that they are more sensitive for the change of heat strength. Also Figure 8 proves that isotropic material provides a very lack sense for heat strength change. But FGMs provide a change in the deflection by changing the amount of heat source strength.

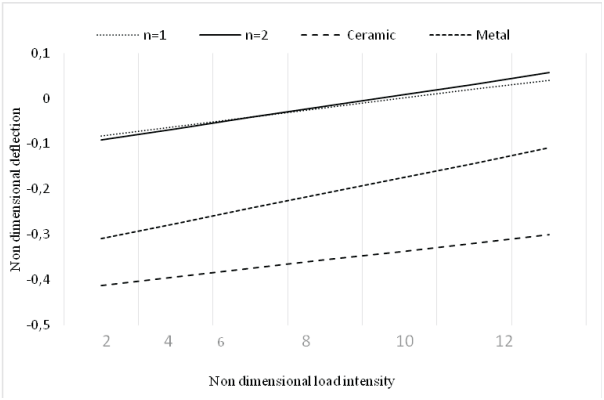

Figure 7 Non dimensional deflection of FGM plate with heat source versus load intensity

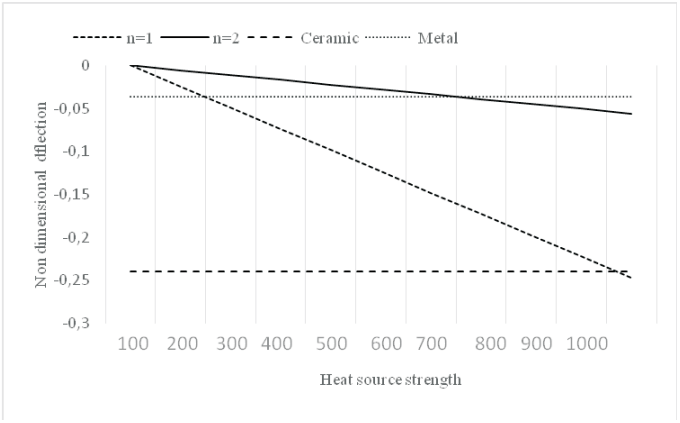

Figure 8 Non dimensional deflections versus the heat source strength

6. Concluding remarks

The behavior of HA/Ti FGM plate under thermal and mechanical loads is investigated and following conclusions are made:

1. The thermal load has dominant effect than mechanical load.
2. Functionally graded materials show a high ability to withstand thermal stresses, which reflect its capacity to operate at high temperatures.
3. The HA/Ti FGMs provide a high resistance to the thermal loading comparing to that of the isotropic materials.

4. The stresses are varied smoothly with comparison to conventional laminated plates without any sort of singularities.

5. The HA/Ti FGM plate is more sensitive for the change of heat strength.

Acknowledgments

Authors are thankful to the I.K. Gujral Punjab Technical University, Jalandhar for their support and guidance during the project.

References

[1] **Sharma, R., Jadon, V. K. and Singh, B.**: A review of the finite element based methods for thermal analysis of functionally graded materials, *J. of IE(India): Series C (under Springer)*, 96, 1, 73–81, **2015**.

[2] **Xu, Y., Wang, L. L. and Zhang, Z.**: Analysis of Convective heat transfer steady thermal stresses in a Zro_2/FGM/Ti-6Al-4V composite plate by FEM, *Int. Joint Conf. on Compu. Sci. and Optimization*, 266–269, **2009**.

[3] **Ramkumar, K. and Ganesan, N.**: Finite–element buckling and vibration analysis of functionally graded box columns in thermal environments, *J. of Mat.: Design and Applications*, 222, 53–64, **2007**.

[4] **Chen,B., and Tong, L.**: Sensitivity Analysis of heat Conduction for functionally graded materials, *Mater. Des.,* 25, 663–672, **2004**.

[5] **Alshorbagy, A. E., Alieldin, S. S., Shaat, M. and Mahmond, F. F.**: Finite Element Analysis of the Deformation of functionally Graded Plates under Thermo–mechanical Loads, *Mathematical Problems in Engineering*, ID 569781, **2013**.

[6] **Ravichandran, K. S.**: Thermal residual stresses in a Functionally Graded Material system, *Mat. Sci. and Engg.*, 20, 269–276, **2001**.

[7] **Kim, K. S. and Noda, N.**:A Green's function approach to the deflection of a FGM plate under transient thermal loading, Archive of *Applied Mechanics*, 72, 127–137, **2002**.

[8] **Cho, J. R. and Oden, J. T.**: Functionally graded material: - a parametric study on thermal–stress characteristics using the Crank-Nicolson-Galerkin scheme, *Comp. methods in appl. mech. & engg.*, 188, 17–38,**2000**.

[9] **Talha, M. and Singh, B. N.**: Thermo–mechanical deformation behavior of functionally graded rectangular plates subjected to various boundary conditions and loadings, *World Academy of Science, Engineering and Technology*, 973–984, **2011**.

[10] **Cheng, Z. Q. and Batra, R. C.**: Three dimensional thermoplastic deformation of a functionally graded elliptic plate, *Composites part B: Engineering*, 31, 2, 97–106, **2000**.

[11] **Tanigwa, Y., Akai, T., Kawamura, R. and Oka, N.**: Transient heat conduction and thermal stress problems of a nonhomogeneous plate with temperature–dependent material properties, *J. of Thermal Stresses*, 19, 1, 77–102, **1996**.

[12] **Praveen, G. N. and Reddy, J. N.**: Nonlinear transient thermoelestic analysis of functionally graded ceramic–metal plates, *Int. J. of Solids and Structures*, 35, 33, 4457–4476, **1998**.

[13] **Alibeigloo, A.**: Exact solution for thermo–elastic response of functionally graded rectangular plates, *Composite structures*, 92, 113–121, **2010**.

[14] **Afsar, A. . and Go, J.**: Finite element analysis of thermoelastic field in a rotating FGM circular disk, *Applied Mathematical Modelling*, 34, 11, 3309–3320, **2010**.

[15] **Tung, H. V. and Duc, N. D.**: Nonlinear analysis of stability for functionally graded plates under mechanical and thermal loads, *Composite Structures*, 92, 5, 1184–1191, **2010**.

[16] **Singha, M. K., Prakash, T. and Ganapathi, M.**: Finite element analysis of functionally graded plates under transverse load, *Finite Elements in Analysis and Design*, 47, 4, 453–460, **2011**.

[17] **Chareonsuk, J. and Vessakosol, P.**: Numerical solutions for functionally graded solids under thermal and mechanical loads using a high-order control volume finite element method, *Applied Thermal Engineering*, 31(2–3), 213–227, **2011**.

[18] **Croce, L. D. and Venini, P.**: Finite elements for functionally graded Reissner-Mindlin plates, *Comp. Methods in Appl. Mech.& Engg.*, 193(9–11), 705–725, **2004**.

[19] **Uysal, M. U.**: Investigation of Thermal and Mechanical Loading on Functional Graded Material Plates, *Int. J. of Mechanical, Aerospace, Industrial and mechatronics Engg.*, 7, 11,1208–14, **2013**.

[20] **Crosby, K. D.**: Titanium–6Aluminum–4Vanadium For Functionally Graded Orthopedic Implant Applications, PhD Thesis, 218, *University of Connecticut*, **2013**.

[21] **Hadi, A., Rastgoo, A., Daneshmehr, A. R. and Ehsani, F.**: Stress and Strain Analysis of Functionally Graded Rectangular Plate with Exponentially Varying Properties, *Indian J. of Mat. Sci.*, **2013**.

[22] **Srinivas, G., Prasad, U. S., Manikandan, M. and Kumar, A. P.**: Simulation of traditional composites under thermal loads, *Research J. of Recent Sci.*, 2, 273–278, **2013**.